JOURNAL OF Materials CHEMISTRY
Feature Article

Design of nanosized structures in sol–gel derived porous solids. Applications in catalyst and inorganic membrane preparation†

Christian G. Guizard,* Anne C. Julbe and André Ayral

Laboratoire des Matériaux et Procédés Membranaires-CNRS UMR 5635, Ecole Nationale Supérieure de Chimie-8, rue Ecole Normale, 34296 Montpellier Cedex 5, France. E-mail: guizard@cit.enscm.fr

Received 6th April 1998, Accepted 27th July 1998

Recent advances in sol–gel processing, with the aim of porous ceramic oxide preparation and applications in catalysis and membrane separation, are reviewed. Recent results from our group in porous solid preparation are presented. Three topics of particular interest are reported which highlight the potential of sol–gel methods to tailor microporous and mesoporous structures in solids, and also the possibility to combine catalyst and ceramic membrane properties. The first one deals with the preparation and the characterisation of supported microporous layers (*e.g.* with pore diameter of less than 2 nm) and the applications linked to ceramic nanofilters. The second topic illustrates improvements expected in sol–gel processing of oxide catalysts and the possibility of forming supported catalytic layers and membranes. The last one has to do with the role of surface active agents in the control of the sol-to-gel transition and in the formation of tailor-made porous structures in oxide materials.

1.0 Introduction

Mesoporous and microporous solids are increasingly being employed in a number of industrially important areas which include catalysis, adsorption processes and membrane separation. Recently Davis and Maxwell edited a review on solid catalysts and porous solids[1] in which was pointed out the importance of catalytic technologies for both economic growth and environmental sustainability. Heterogeneous catalysis appears as a major concern in the development of new catalyst systems for oil refining, chemical synthesis, natural gas conversion and environmental technology. Adapted catalysts are based on mesoporous and microporous solids with or without added metals. The important research and development activity on microporous and mesoporous materials for molecular sieve and adsorbent applications should also be emphasised. The discovery of mesoporous molecular sieves is certainly the most remarkable advance in this field. These materials exhibit structured inorganic frameworks with pores large enough (2–10 nm) to be used in a wide range of application including shape-selective catalysis, sorption of large organic molecules, chromatographic separations, and use as hosts to confine guest molecules and atomic arrays. The mesoporous structure of gels derived from colloidal sols of oxide and clay particles has also been described in the literature as a basis for preparing adsorbents with controlled and uniform pore geometry.[2]

Another important concern in the field of porous materials is the notable development of inorganic membranes over the past decade. A recent book edited by Burggraaf and Cot deals with fundamentals of inorganic membrane science and technology.[3] The current industrial applications of inorganic membranes mainly focus on liquid separations. In the meantime the market for gas separation and related applications is considered to be potentially very important. Regarding future developments, the catalytic membrane reactor concept is certainly the most exciting and promising idea in the area of inorganic membranes. Combining reaction and separation in the same unit often creates a synergy and many reports agree that acceptance of catalytic membrane reactors on a commercial scale will arise within the next ten years.

Most of the above related applications concern porous ceramic oxide materials. Today the demand in catalysis and separation applications is for selective materials able to perform reaction and separation of a wide range of salts, organic molecules, gases and vapours. The efficiency of these catalytic and separation processes strongly depends on the pore size of the used materials (catalysts, adsorbents or membranes) in relation to the size of the processed molecules and ions. Consistently the control of the porous structure (pore size, pore volume and surface area) is of prime importance in the development of more specific materials. The thermal stability of such materials is also a crucial parameter for the applications listed above. Most of the catalysts, adsorbent or inorganic membranes can be described as ceramic nanophase materials in which ultrafine grain sizes and a large fraction of the interfacial volume are responsible for a variety of novel and potentially advantageous properties and characteristics compared to those of conventional materials. This new class of materials results from the emphasis of some new ceramic synthesis methods like the sol–gel process.

The sol–gel process presents inherent advantages for the preparation of porous ceramic oxides, because the nanostructure of the derived materials can be controlled together with their porous structure (*e.g.* formation of mesopores or micropores). Other quoted advantages of sol–gel processing are compositional homogeneity and the ability to prepare shaped materials such as spherical particles, fibres and thin films. Depending on the method used, colloidal or polymeric, two main gel structures can be obtained which are described in the literature[4] as: (i) physical gels in which steric or electrolytic effects in the sol dominate gel formation. The main characteristic of this type of gel is the way in which individual particles contained in the sol can be arranged during the process. These gels are rather concerned with aqueous media; and (ii) polymeric gels in which the relative rates and extents of chemical reactions lead to cluster polymerization and interpenetration during gel formation. In this case organic media are preferred.

The scope of this paper is to review innovative developments in sol–gel processing of ceramic oxide nanophase materials in relation to the preparation of both catalysts and membranes. Three topics of particular interest are reported which highlight the potential of sol–gel methods to tailor microporous and mesoporous structures in solids, and also the possibility to combine catalyst and ceramic membrane properties. The first

†Basis of the presentation given at Materials Chemistry Discussion No. 1, 24–26 September 1998, ICMCB, University of Bordeaux, France.

one deals with the preparation and the characterisation of supported microporous layers (*e.g.* with pore diameter of less than 2 nm) and the applications linked to ceramic nanofilters. The second topic illustrates improvements expected in sol–gel processing of oxide catalysts and the possibility of forming supported catalytic layers and membranes. The last one has to do with the role of surface active agents in the control of sol-to-gel transition and in the formation of tailor-made porous structures in oxide materials.

2.0 Microporous materials and membranes formed from nanoparticulate sol–gel systems

2.1 General aspects of microporous membrane preparation and characterisation

The sol–gel process is one of the most appropriate methods for the preparation of microporous oxide layers. Two sol–gel routes, polymeric or colloidal, can be used to prepare supported ceramic membranes in which the porous structure is mainly influenced by the different steps involved in the process even at the very first stage of precursor chemistry. The first stage in the sol–gel process consists of the preparation of a sol using molecular precursors, either metal organics (preferentially metal alkoxides) or metal salts. In both cases condensation reactions occur at the sol stage with formation of clusters or colloids which collide at the final stage to form the gel. In the case of membrane formation, coating of the active layer has to be carried out at the sol stage with rheological behavior adapted to the porous substrate chosen as membrane support. Actually, inorganic membranes are formed following a three-step thermal treatment of freshly cast gel layers. At first, the supported gel layer is dried at low temperature ($<100\,^{\circ}C$). Then the dried layer is fired to an intermediate temperature (*ca.* $350\,^{\circ}C$) in order for residual organic groups and carbon to be burned out. Finally the consolidation of the membrane is performed through viscous or conventional sintering depending on the amorphous or crystalline structure of the membrane material. During sol–gel processing of inorganic membranes, sols and gels evolve in a different way depending on the category of the precursors used. This evolution has a great influence on the porous structure of the final membrane materials.

On the one hand, polymeric gels formed in organic media from interpenetrated clusters lead to microporous membrane materials[5,6] as shown in Fig. 1. The problem with this category of membrane is that microporous volumes remain very low; this is a major limitation for liquid filtration and particularly for nanofiltration application of these materials. On the other hand, in particulate sol–gel systems, the corresponding sols contain individual particles surrounded either by a steric barrier or an electrical double layer responsible for interparticle repulsion and sol stability.[7] A strong steric effect or a high electrostatic repulsion barrier between particles at the sol stage provides a dense packed bed of particles during gel formation close to a perfect arrangement of spheres (green density $d=0.74\ d_{th}$). In this case materials with a rather low porosity ($\leqslant 30\%$) and capable of readily densifying at high temperature are generally obtained. For weaker interactions, a partial aggregation of particles can occur in the sol and consequently a high porous volume is obtained in the gel as well as in the final material. These two effects, which are shown in Fig. 2, can be exploited for the preparation of ceramic membranes with a controlled microporous or mesoporous structure.[7] Thermal treatment is another parameter which can affect the porous structure of the final membrane material. In the case of materials obtained from particulate sols, a grain growth phenomenon is generally found to be responsible for an increase of pore size corresponding to the evolution of residual voids between the sintered particles. The classical physical gels

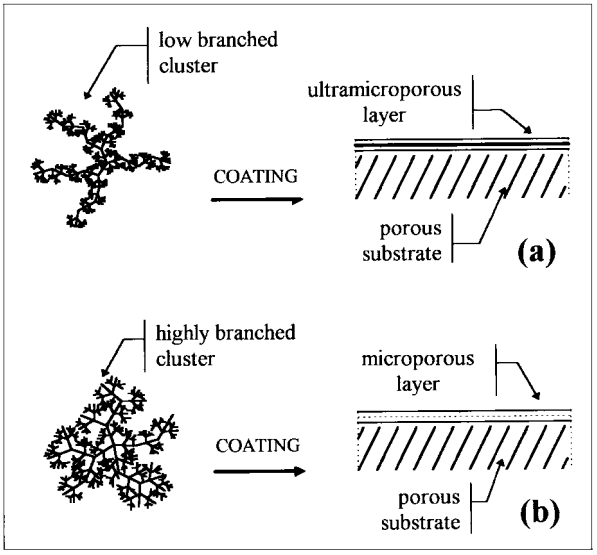

Fig. 1 Influence of cluster structures in polymeric sols on the porosity of coated layers: (a) packing of interpenetrated low branched clusters, (b) packing of non-interpenetrated highly branched clusters.

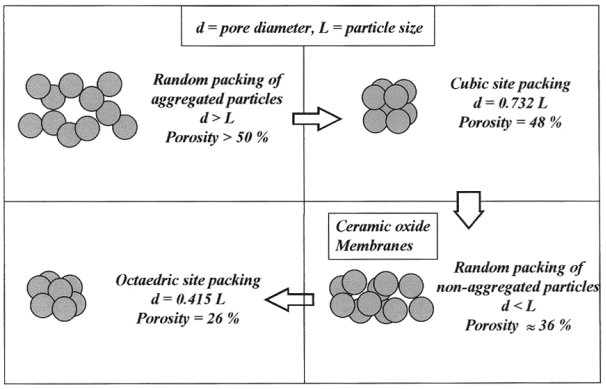

Fig. 2 Packing density of colloidal particles in solids obtained from physical gels.

formed from colloidal particles in aqueous media yield membrane materials with 30–35% porosity (Fig. 2) and with pore sizes in the intermediate range between mesopores and micropores. A specific problem arises in the case of microporous ceramic membranes. Indeed, two main conditions exist in order to prepare nanophase ceramics exhibiting a connected microporosity with a narrow pore size distribution. The first one is to prevent particle aggregation at the sol stage responsible for the formation of large and polydispersed sintered grains yielding a residual mesoporosity, the second one is to preserve individual grains of less than 10 nm all along the process up to the sintered ceramic. This is possible by using a new preparation route which consists of the formation of nanoparticulate stable sols in organic solvents. In this case the particles, which are less than 10 nm in size, consist of a mineral core surrounded by an organic shell which prevents aggregation (Fig. 3) and allows the formation of a connected microporous structure with porosity in the 20–30% range. An example dealing with the preparation of a microporous zirconia layer according to this method is given hereafter.

The characterisation of the porous structure of supported thin films and membranes is a complex problem, since total porosity, pore size and pore size distribution must be analysed. A quite difficult problem is the characterisation of microporous materials[8–10] for which thermodynamic laws are no longer valid because of very strong interactions between intrusive fluids and pore walls. The methods based on gas adsorption

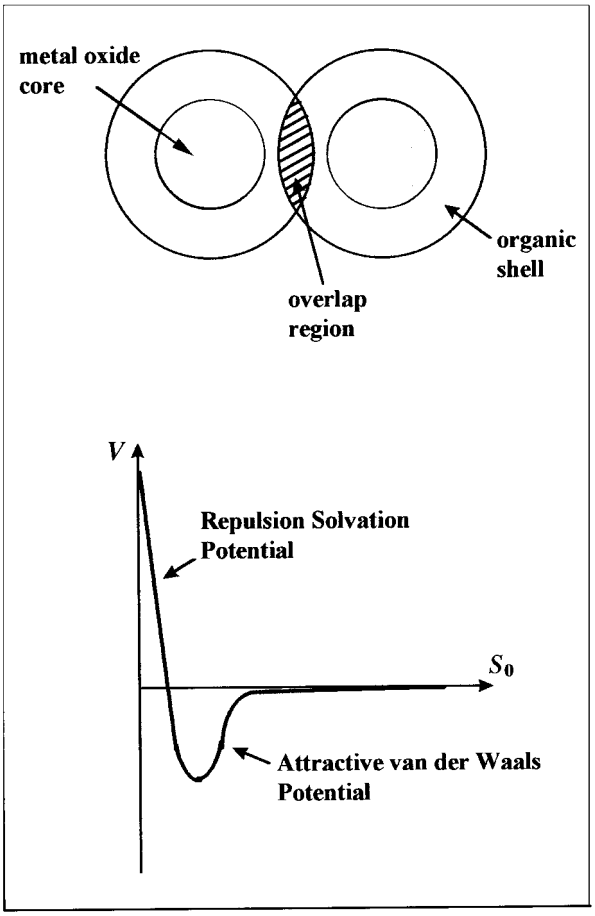

Fig. 3 Interaction and corresponding potential (V) between steric barriers due to the presence of organic shells around ceramic particles.

are the most convenient for the study of microporous materials. The conventional apparatus uses volumetric measurements of the adsorbed gas quantities.[11] In the case of supported thin films, the amount of porous layer which can be introduced in a standard-size sample cell is often too small to be correctly characterised. Other types of adsorption equipment were therefore developed, like the surface acoustic wave device[12] and a device based on the measurement of the refractive index by ellipsometry.[13] However these techniques require specific conditions concerning the nature of the substrate. In the first case, the substrate must be piezoelectric, while in the second case, the layer must be transparent and the refractive index of the dense substrate must be quite different from that of the layer. In other respects, each substrate exhibits specific surface properties which can influence the final characteristics of the deposited coatings. In a recent work we combined adsorption measurements and ellipsometry for the characterisation of supported microporous silica layers.[14] Both silica layers and the corresponding bulk silica materials were prepared by the sol–gel polymeric route using tetraethoxysilane as the starting material. This work led to the conclusion that during the drying step the support has a great influence on the porous structure formation of the coated layer. The support prevents shrinkage of the thin layer resulting in a higher porosity compared to the bulk material. Further modification or adaptation of these techniques must be completed in order to better characterise the porous structure of supported membranes, particularly microporous membranes.

2.2 Preparation of a zirconia nanofilter from a nanoparticulate organic sol

Starting from the above considerations it is possible, from a nanoparticulate sol, to create a connected microporous structure in supported ceramic films. Such materials offer attractive properties when used as ceramic nanofilters.[15] Ceramic nanofilters are being recognised as of growing importance owing to increasing demands for membrane systems which are able to separate ions and small molecules in harsh working conditions (high temperature, extreme pH, organic solvent media). Regarding the problem of aggregation, a solution has been to generate steric repulsion in organic media through the interaction of organic shells preventing close contact between nanoparticles in the sol, Fig. 3.

Taking into account the role of chelating agents as blocking functional groups in metal alkoxide condensation[16] a supported microporous zirconia layer has been obtained from a nanoparticulate organic sol. Zirconium isopropoxide was used as the ceramic precursor to synthesise the organic particulate sol.[17] In order to avoid the precipitation of non-homogeneous hydroxide particles during the hydrolysis step, the alkoxide reactivity was modified by a strong complexing ligand, acetylacetonatee (acac). Hacac reacts with the alkoxides to form mixed complexes which have different physico-chemical properties and, more importantly, which are more difficult to hydrolyse than alkoxy groups:[18]

$$Zr(OR)_4 + Hacac \rightarrow Zr(OR)_3(acac) + ROH$$

Then this ligand acts as a functionality blocker when substoichiometric hydrolysis ratios are used. Consequently, a Hacac/M molar ratio greater than 1 was used to prevent precipitation and led to a stable nanoparticulate sol prepared in air without any precipitation. Here the stability of nanoparticles in the sol results from the interacting organic shells formed with the acac groups as shown in Fig. 4.

The supported zirconia layer obtained after sintering at 500 °C exhibited a tetragonal crystalline structure and revealed a very fine texture when observed by TEM. In the case of a Zr/Hacac molar ratio = 2, a mean grain size of about 6 nm was measured. Powder X-ray diffraction (Scherrer's formula) was used for the determination of an average individual crystal size. Results are consistent with particle size observed by TEM in the supported membrane, Fig. 5. In this membrane packing of the nanoparticles results in a pore diameter of 1.4 nm and a porosity of 18%.

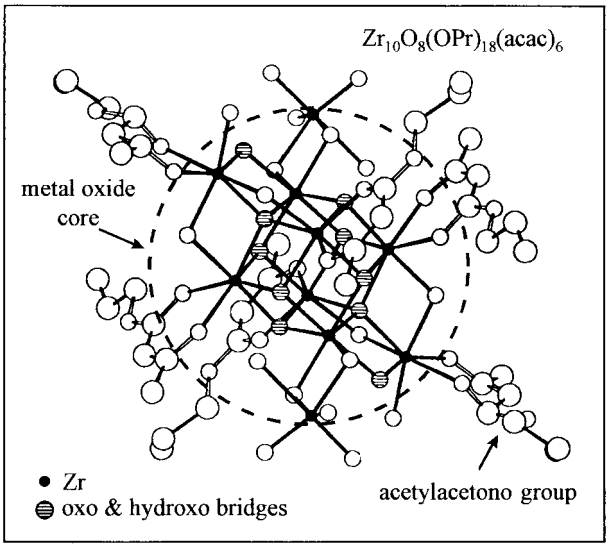

Fig. 4 Cluster formed from condensation of acetylacetone (Hacac) modified zirconium isopropoxide; acac groups are at the periphery of the cluster as an organic shell and prevent interpenetration of clusters which behave as individual nanoparticles.

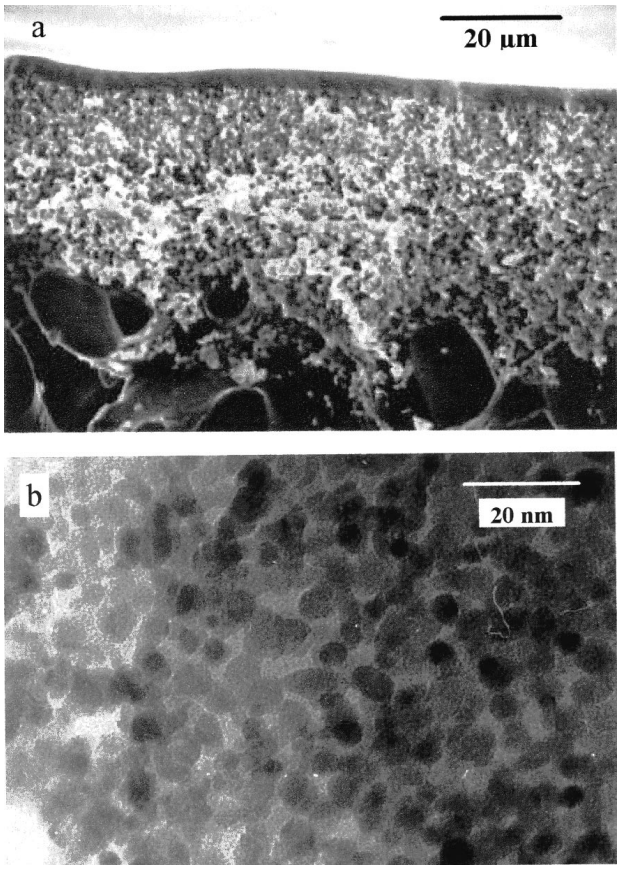

Fig. 5 Electron microscopy images of the active zirconia layer of a ceramic nanofilter prepared at 500 °C from a sol of Hacac modified zirconium alkoxide precursor. (a) SEM cross-section image of the supported zirconia layer, (b) TEM image of the zirconia nanoparticles constituting the zirconia layer.

3.0 Catalytically active nanophase materials from the sol–gel process

The sol–gel process is also of particular interest for designing catalytically active materials with specific properties and/or with improved performances compared to those of classical catalysts. It allows preparation of catalytically active materials which can be directly cast in/on supports at the sol stage. This is a great advantage for catalytic membrane development.[19] The classical synthesis methods for conventional catalysts often start from salts or oxide precursors and involve precipitation, impregnation or even solid/solid reactions. These methods are usually not adapted to a homogeneous casting of the catalyst on a support and may lead to limited specific surface areas and to a heterogeneous distribution of active species. The sol–gel process, starting from a homogeneous distribution of the precursors at the molecular level, can in many cases improve these specific criteria. Indeed a large range of methods and precursors can be investigated to obtain the required powders or film-shaped materials either as a pure catalyst or homogeneously doped or dispersed in a matrix. Furthermore, the specificity of the process can lead to original materials which can help in a better understanding of the catalytically active sites in a specific catalyst. Two examples showing the potential of the sol–gel process for catalyst synthesis are described in the following sections.

3.1 VMgO catalysts prepared from original metallo-organic precursors

The method classically used to prepare conventional VMgO catalysts for the oxydehydrogenation of propane involves the precipitation of $Mg(OH)_2$ and its impregnation with a solution of ammonium metavanadate.[20,21] The synthesis of original metallo-organic molecular precursors has been attempted in order to obtain a homogeneous liquid, adapted to casting and being a precursor of a pure VMgO catalyst, with a controlled V/Mg ratio, a high specific surface area and a high catalytic activity (dispersion of active sites). A functional magnesium alkoxide $Mg(OCHCH_3CH_2OCH_3)_2$ has been synthesised by direct reaction between magnesium and 1-methoxypropan-2-ol[22] and reacted with a new original vanadium oxoalkoxide $VO(OCHCH_3CH_2OCH_3)_3$ prepared by reaction of ammonium metavanadate with 1-methoxypropan-2-ol. The reaction leads to the formation of $(OR)_{n-1}VOMg(OR)_{m-1}$ species. This heterometallic compound can be easily cast on a support, hydrolysed, dried in vacuum at room temperature and finally fired at 600 °C in air to lead to the final VMgO catalyst with a controlled V/Mg ratio. Apart from the fact that this specific method is well adapted to catalyst casting on a support (*e.g.* for catalytic membrane reactor applications), the derived VMgO powders have been found to exhibit original specific characteristics when compared to conventional VMgO catalysts derived from precipitated $Mg(OH)_2$. These characteristics concern both the textural properties of the catalysts (high specific surface area: 110 m^2 g^{-1} at 14 wt% V, round particles of about 25 nm instead of platelets for conventional catalysts) and also their structural characteristics (delayed crystallisation of $Mg_3V_2O_8$, high dispersion of amorphous vanadium species on the surface of MgO particles). Fig. 6 compares the morphology of the VMgO powders (14 wt% V) obtained at 600 °C from the $Mg(OH)_2$ salt precursor[21] and from the above-mentioned alkoxides. The specific characteristics of the alkoxide derived catalyst, attributed to a high homogeneity of V and Mg species distribution in the molecular precursor, induce attractive catalytic properties for the oxydehydrogenation of propane. Some preliminary results have

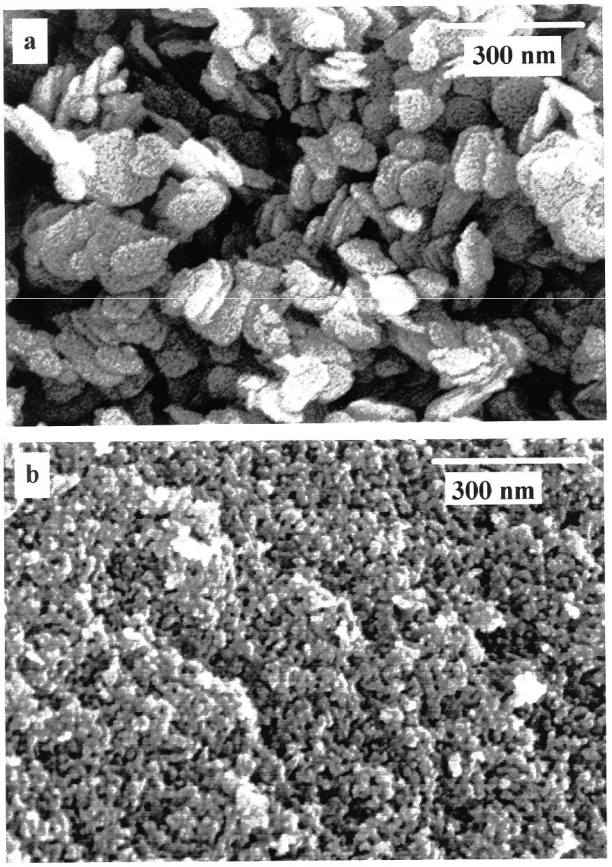

Fig. 6 FESEM observation of VMgO (14 wt.% V) catalytic powders obtained at 600 °C from: (a) $Mg(OH)_2$ salt precursor (S_{BET} = 90 m^2 g^{-1}), (b) novel metal alkoxides (S_{BET} = 110 m^2 g^{-1}).

been reported recently.[23] VMgO powders with various V/Mg ratios are currently being investigated and should help in a better understanding of the nature of the catalytic sites active for the oxydehydrogenation of propane. The corresponding optimised mesoporous membranes will be tested as contactors in a catalytic membrane reactor configuration (European Joule program JOE3-CT-95 0022).

3.2 Synthesis of CeO_2 based materials for DeNOx applications

Most of the three-way catalysts (TWCs) currently used for car exhausts are made with a washcoat (on honeycomb supports) of a mixture of oxides, namely Al_2O_3 and CeO_2, which is impregnated with Pt, Pd or Rh salts.[24] The main problems related to classical TWCs lie both in the elevated price of noble metals and in the instability of the catalysts upon use (oxide sintering and metal aggregation).[25] The goal was in this case to investigate sol–gel methods and precursors providing the best conditions for the preparation of efficient CeO_2 based catalysts with a high specific surface areas at 1000 °C and from precursors able to be directly cast on supports. A sol–gel preparation method was used, starting from $Ce(acac)_3 \cdot xH_2O$ and $Al(O^sBu)_3$ as ceria and alumina precursors, respectively. Hydrolysis and condensation of the precursors in the presence of water was carried out in hexylene glycol at 100 °C for 24 hours with the following weight% composition for the initial sol: precursors 40/hexylene glycol 50/water 10. Gel formation depends on the precursor molar ratio, for $Al(O^sBu)_3/Ce(acac)_3 \cdot xH_2O > 0.25$ gel formation occurred immediately after water addition. The as-formed gels were heat treated at 1000 °C and the resulting powders analysed by X-ray, FESEM and N_2 adsorption–desorption. Different $Ce(acac)_3 \cdot xH_2O/Al(O^sBu)_3$ ratios were investigated. The homogeneous dispersion of CeO_2 in the alumina matrix was found to prevent fast growth of cerium oxide crystallites with temperature when the CeO_2 content in the final material was less than 25 mol%. The evolution of the powder specific surface areas *versus* CeO_2 content and firing temperature is reported in Fig. 7.

Specific surface areas higher than 100 $m^2\ g^{-1}$ have been obtained at 1000 °C for CeO_2–Al_2O_3 based materials containing less than 25 mol% CeO_2. When the CeO_2 content was too high ($\geqslant$47 mol%) the dispersive effect of alumina decreased and S_{BET} at 1000 °C was lower than 10 $m^2\ g^{-1}$. The SEM observation of the powders with 25 mol% of CeO_2 (Fig. 8a) showed that the grain sizes were always homogeneous and never exceeded 30–40 nm at 1000 °C. Without any alumina in the powder the grain sizes were larger than 200 nm at 1000 °C, and in the case of alumina alone the grain sizes were about 15 nm at 1000 °C. It should be noted that the alumina matrix remained amorphous up to 700 °C, as only the sole CeO_2 diffraction lines were detected. At 1000 °C, some poorly defined diffraction lines of γ-Al_2O_3 began to appear. This delayed crystallisation of alumina was attributed to an effect of CeO_2, as the structure of alumina prepared without any additive was already crystalline at 450 °C. The CeO_2 crystallite sizes determined from the X-ray diffraction peak widths were smaller than 20 nm.

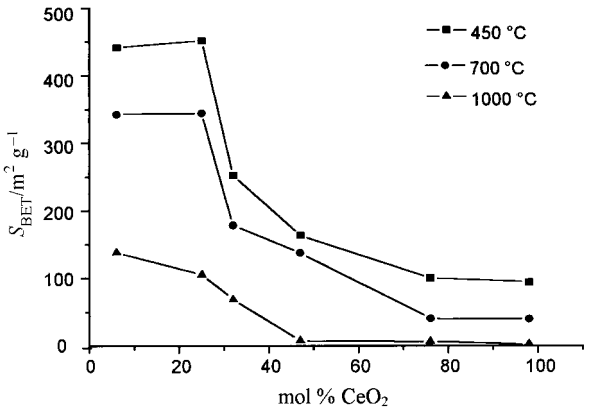

Fig. 7 Evolution of the specific surface area in CeO_2–Al_2O_3 powders as a function of the CeO_2 content and firing temperature. Sol–gel organic route from $Ce(acac)_3 \cdot xH_2O$.

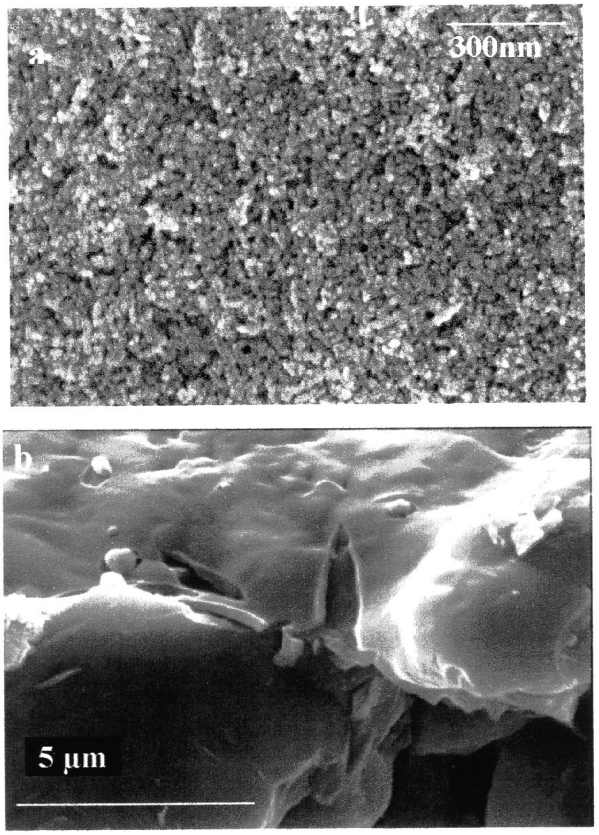

Fig. 8 Morphological aspect of CeO_2–Al_2O_3 based $DeNO_x$ catalyst: (a) powders heat-treated at 1000 °C, (b) corresponding honeycomb supported layer.

The corresponding sols lead to homogenous layers when cast on honeycomb supports, Fig. 8b. High temperature ageing tests are in progress in order to check the structural stability of the derived TWC catalysts. The sol–gel route previously described is also currently being investigated for the direct insertion of zirconia (forming a solid solution with ceria and enhancing its redox properties) and of Pd catalysts at the sol stage (European Brite EuRam program BRPR-CT 96 0290).

4.0 New methods based on amphiphilic media to tailor porous structures in sol–gel derived solids

4.1 Interest of surface active agents for the control of pore formation

Surface active agents represent a specific variety of additives which has been recently investigated in sol–gel processing and not only to limit gel cracking. Indeed, one of the other interests of such additives concerns the control of the hydrolysis step of highly reactive alkoxides, such as titanium alkoxides, by the use of reverse micelle sol–gel systems.[26] Another utilisation under investigation in our group is the modification of gel porous structures when surfactant molecules are added after the hydrolysis of an alkoxide.[27] As shown in Fig. 9, the surfactant molecules introduced in the reaction medium interact with growing clusters and their role is in this case the

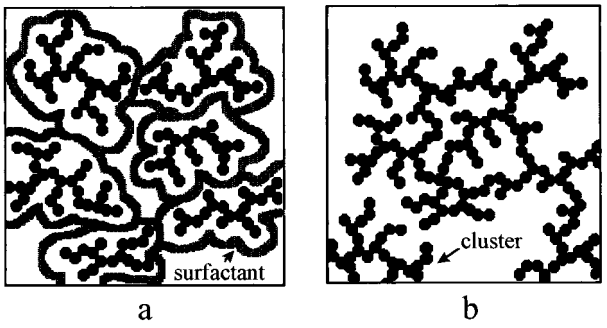

Fig. 9 Schematic representation of the role of non-ionic surfactants in the limitation of cluster growth and aggregation: (a) gel formation with added surfactants, (b) gel formation in the absence of surfactants.

limitation of both interpenetration and condensation between clusters. In addition to the material pore sizes and pore volume, it is also of particular interest to control the pore connectivity which is an important parameter affecting the material permeability. Nakanishi *et al.*[28] used the spinodal decomposition of sol–gel solutions into two phases, one rich in solvent and the other rich in polyethylene oxide and inorganic compounds, to produce dried gels with interconnected pores in the micrometer range. Unfortunately this method cannot be extended to the nanometer range and the templating approach is much more attractive by using removable individual templating units or interconnected networks. At the nanometer scale the lyotropic liquid crystal mesophases appear as very attractive systems which can produce removable interconnected networks. Moreover the crystalline structure of these templates can direct the growth of the inorganic network and leads to the formation of ordered structure and porosity. The periodicity of the structures induces monodispersed pore sizes and uniform connectivity of both the porous and solid networks.[29] Lyotropic liquid crystals are usually lamellar, hexagonal and cubic phases (Fig. 10). They are obtained by a self-assembly process of surfactant molecules for intermediate compositions in the water–surfactant binary phase diagrams. The sizes of the constituent units, *i.e.* the amphiphilic aggregates, usually range from 2 to 10 nm and are susceptible to direct the formation of inorganic networks with an ordered porosity from the supermicroporous domain (>0.7 nm) up to the mesoporous domain (>2 nm).

There is currently considerable interest in this new field of material science which integrates both a biomimetic approach (biomineralisation processes) and the concept of nanochemistry. In 1992 researchers at Mobil published a synthesis of mesoporous molecular sieves using the templating effect of lyotropic liquid crystal mesophases.[30,31] The aluminosilicate or silicate materials M41S were prepared by hydrothermal treatment of solid or molecular precursors of alumina and silica in the presence of cationic surfactants of alkyltrimethylammonium halide type. As in the case of zeolites, micrometer

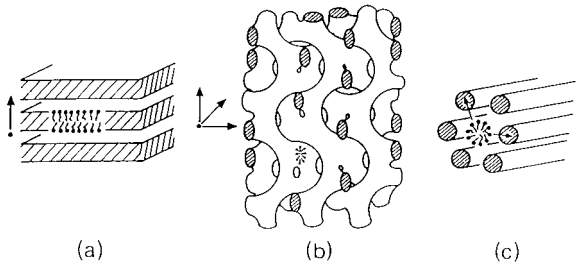

Fig. 10 Drawing of three lyotropic liquid crystal structures: (a) lamellar, (b) bicontinuous cubic (space group *Ia*3*d*) viewed along the ⟨100⟩ direction, (c) hexagonal. J. Charvolin, *Prog. Colloid Polym. Sci.*, 1990, **81**, 6 (reproduced with permission).

sized 'crystallites' can be obtained; a firing treatment removes the surfactant aggregates and liberates the ordered porosity. The initial mixture composition controls the structure (lamellar, hexagonal or cubic) of the mesophase. The main material labelled MCM41 exhibits a hexagonal ordered porous texture. The pore sizes are directly controlled by the length of the surfactant alkyl chain and ranges between 1.8 and 10 nm. Monnier *et al.*[32] explained the co-operative process of oxide polymerisation and mesophase formation by the evolution of coulombic type interactions between the surfactant polar head and the growing silicate oligomers. Subsequent studies[33–38] showed that the synthesis of a silica network in ordered amphiphilic media could also be obtained by sol–gel routes at room temperature, under atmospheric pressure and with other types of surfactant, anionic or non-ionic. In contrast to the M41S type structured mesoporous solids our main objective has been to create, during the sol-to-gel transition, ordered microporous structures in oxide materials using the directing effect of lyotropic liquid crystal mesophases.[33–36] Moreover these materials have been shaped as continuous supported thin films in view of membrane applications for liquid and gas separation.[34] We first worked on ordering of porous structures in sol–gel derived silica materials with further investigation of other metal oxide systems like alumina. Beyond the preparation of the ordered structures an important improvement in porous membrane characteristics can be expected in terms of sharp control of pore tortuosity. Tortuosity is one of the important structural parameters which governs membrane permeability. As a prospect we relate at the end of this paper some preliminary works on the orientation of ordered domains in silica supported layers with the aim to prepare membranes with low tortuosity.

4.2 Control of residual porosity in silica materials derived from polymeric gels

Based on the same concept as for zirconia nanoparticulate organic sols, an interesting way to tailor the microporous structure in silica materials and membranes is based on hindered cluster formation at the sol stage (Fig. 9) using non-ionic surfactants. In this approach, non-ionic surfactants, alkylaryl polyether alcohols Triton (TX) of different molecular weights ($X=1$–30) were added to tetraethoxysilane sols (molar composition: $TEOS/C_2H_5OH/H_2O/HCl=1/4.5/4/0.02$). On the basis of sol and gel characterisation (gelation time, ^{29}Si NMR, QELS, SAXS, thermoporometry) and material characterisation (FESEM, N_2 adsorption, FTIR) the effect of surfactant chain length (X) and TX/TEOS ratio on derived sols, gels and ceramic materials has been explored.[27] In other respects thermoporometry is a method which is well adapted to the study of the evolution of mesoporosity in wet gels. We have shown,[39] using this technique, that the Triton X surfactant molecules prevent interpenetration and further condensation of clusters in the above-mentioned sols. Because surface active agents are susceptible to interaction with silica oligomers derived from TEOS by van der Waals forces or by interaction with OH groups, the formation of an organic shell made of surfactant molecules between the clusters can be assumed. On the other hand the possibility of micelle formation during drying, by exceeding the surfactant cmc, cannot be set aside but there was no experimental evidence of that. Anyway, in both cases the resulting steric hindrance should limit further condensation of clusters during sol ageing. This is confirmed experimentally by reduced bonding between clusters which explains the formation of more stable sols with longer gelation time and a reversible sol-to-gel transition upon gel shaking. During the heat treatment (450 °C, 2 h) there is formation of a homogeneous microporous material due to the elimination of the surfactant molecules in contact with the silica gel matrix. N_2 adsorption experiments revealed that N_2 (kinetic diam-

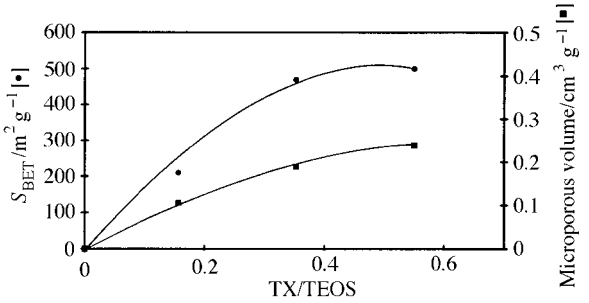

Fig. 11 Evolution of specific surface area and microporous volume of silica materials *versus* the molar ratio TX/TEOS.

eter = 3.96 Å) does not penetrate the porous structure of SiO_2 materials prepared without a surface active agent. When surfactants were used, type I isotherms were obtained which are characteristic of microporous materials. The mean hydraulic pore radius R_H (estimated by the MP method) can be varied between 3.2 and 7.0 Å. This parameter is slightly affected by the TX/TEOS molar ratio but increases with the surfactant chain length X. Surfactant addition greatly increases the pore volume and specific surface area of silica materials. As shown in Fig. 11, these two parameters, in the case of X = 3, reach a maximum (S_{BET} = 500 m^2 g^{-1}, Micropore volume = 0.239 cm^3 g^{-1}, 35.5% porosity) for TX/TEOS = 0.55. Fig. 12 shows the evolution of the pore volume and specific surface area as a function of the surfactant chain length X for a ratio TX/TEOS = 0.55. The curves seem to reach a plateau for X higher than 10. In fact with long chains, larger pore sizes and wider distributions were obtained, whereas to obtain small pores with a sharp distribution, a high pore volume and specific surface area, X values of 3 to 10 and TX/TEOS ratio of 0.55 were preferred. This kind of sol was successfully used to prepare supported microporous silica membranes.[27] A thorough investigation of residual OH groups by FTIR spectroscopy[40] showed another attractive feature of this type of material related to the presence of single OH surface groups at high temperature. These single OH groups (typical sharp IR absorption band at 3744 cm^{-1}) were clearly distinguished on FTIR spectra from adjacent OH groups (broad absorption bands at 3670 and 3500 cm^{-1}) which completely disappeared upon firing at 600 °C whereas the band at 3744 cm^{-1} remained. The unusual presence of these groups is specifically due to the presence of surfactant molecules in the sol and to their interaction by hydrogen bonding with the silica based clusters. At the sol and gel stages, these OH groups are 'protected' by the surfactant hydrophilic head. This interaction is maintained till the surfactant thermal decomposition, between 200 °C and 300 °C, when single OH groups are liberated. These groups have been shown to be relatively distant from each other because of surfactant steric hindrance and cannot easily condense as in classical sol–gel derived silica. This original surface characteristic of materials derived from TX–TEOS sols should

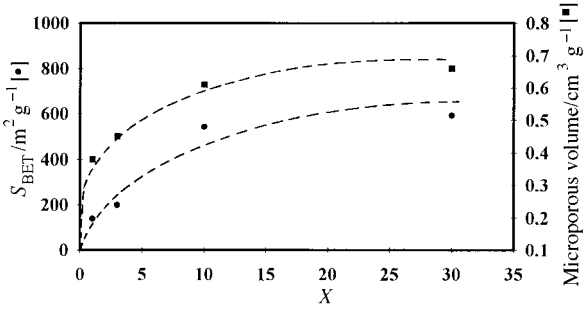

Fig. 12 Evolution of specific surface area and microporous volume of silica materials *versus* surfactant chain length.

be of importance for material reactivity: ionic exchange, organic grafting, specific interactions with gas or liquid phases.[41]

This type of sol prepared in the presence of surfactant is also well adapted for preparing homogeneous dispersions of metals in a silica matrix. An example is reported[39] relating the dispersion of a platinum salt ($PtCl_4$) in a TX–TEOS sol. Thermoporometry of the derived gels showed that the effect of $PtCl_4$ is opposite to the effect of Triton X and leads to gels with a higher crosslinking degree. The conjunction of the steric hindrance and rigidity effects of Triton X and $PtCl_4$ respectively produces rigid gels in which the surfactant molecules are trapped. This is an original method to prepare highly microporous SiO_2/Pt supported membranes which contain a homogeneous dispersion of catalytically active nanosized Pt particles.[41]

4.3 Templates based on a removable interconnected network. Structure directing effect of lyotropic liquid crystal mesophases

In a previous work, silica gels with ordered microporosity were prepared using short length cationic surfactant molecules which show less ability to form lyotropic mesophases.[33,36] The sol compositions (Table 1) were based on a silica precursor, tetramethoxysilane, mixed with a series of cationic surfactants of alkyltrimethylammonium bromide type: $C_xH_{2x+1}(CH_3)_3N^+Br^-$ (x = 8, 10, 12, or 14) and water. In these systems gelation of the silica network and mesophase formation occur simultaneously. The X-ray diagrams (Fig. 13a,c) of two wet gels prepared according to this method (for x = 8 and x = 14) can be assigned to hexagonal and lamellar phases respectively. The large Bragg spacing d_{100} can be related to the existence of a liquid crystal structure and its value varies with the length of the chain of the used surfactant molecule. In the investigated surfactant series, Table 2, the wet

Table 1 Composition of the silica sols synthesised in presence of alkyltrimethylammonium bromides, $C_xH_{2x+1}(CH_3)_3N^+Br^-$ (with x = 8, 10, 12, or 14)

Reagent	Surfactant	Tetramethoxysilane	Water
Weight %	21	12	67
Addition order	1	2	3

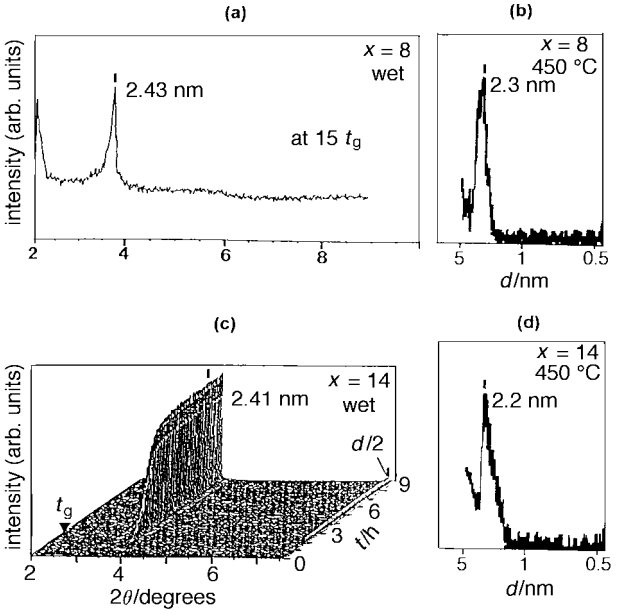

Fig. 13 X-Ray patterns of various wet and thermally treated gels: (a) x = 8, wet gel; (b) x = 8, gel treated at 450 °C under nitrogen; (c) x = 14, wet gel; (d) x = 14, gel treated at 450 °C under nitrogen.

Table 2 Textural properties of the thermally treated gels calculated assuming given mesophase structures

Gel	ϕ_p	d_{100}/nm	d_c/nm	S_M/m^2 g^{-1}	S_{BET}/m^2 g^{-1}	ΔS/m^2 g^{-1}	D/nm
$x=8$	0.55	2.3	2.1	1074	1260	186	33
$x=10$	0.55	2.8	2.5	883	1040	157	39
Gel	ϕ_p	d_{100}/nm	w_p/nm	S_M/m^2 g^{-1}	S_{BET}/m^2 g^{-1}	ΔS/m^2 g^{-1}	D/nm
$x=12$	0.58	2.0	1.2	1082	1100	18	366
$x=14$	0.58	2.2	1.3	1033	1090	57	120

gels exhibit a hexagonal structure for the lower values of x (8 and 10) whereas for higher values of x (12 and 14) the wet gels are lamellar. After drying and firing at 450 °C under nitrogen, a broad diffraction peak is observed in the X-ray patterns (Fig. 13b,d). The decrease of d_{100} from the wet to the thermally treated gels has been attributed to a shrinkage of the material during the drying step at low temperature and to the condensation of reactive groups of the silica network. Taking into account the sharpness of the diffraction peaks for the wet gels compared to an important broadening of the diffraction peaks after heat treatment it can be stated that the size of the ordered domains is reduced during the transition from the wet to the thermally treated gel. Final ordered domains of about 20 nm in size were determined using the Scherrer relation.[42] The final size of these domains is small compared to the size of the liquid crystal cells implied in the formation of the material. This small size and the probable random orientation of the ordered domains could explain the limited collapse of the lamellar structures upon heating at 450 °C.

The main remarkable results (Table 2) obtained with these materials exhibiting a directed porous structure can be summarised as follows. The BET specific surface area, S_{BET}, and the total porosity are very large, more than 1000 m^2 g^{-1} and around 60% respectively. The calculated diameter of the cylindrical pores, d_c, for the hexagonal gels and the calculated width of the slit-like pores, w_p, for the lamellar gels are consistent with the size of the micropores experimentally determined by the MP[43] and Horvath–Kawazoe[44] methods. Fig. 14 shows that the average hydraulic diameter, $2r_h$, and the average Horvath–Kawazoe diameter, d_{HK}, are almost proportional to x, the number of carbons of the alkyl chain

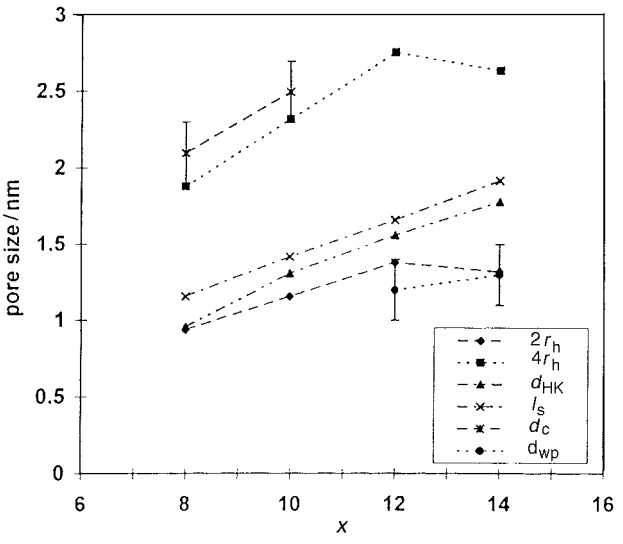

Fig. 14 Measured and calculated average size of pores *versus* x, the number of carbons in the alkyl chain of the surfactant. (a) $2r_h$ with r_h the measured hydraulic radius; (b) $4r_h$; (c) d_{HK}, measured average Horwath–Kawazoe diameter; (d) l_s, calculated length of the surfactant molecule; (e) d_c, calculated diameter of the cylindrical pores in the hexagonal structure; (f) w_p, calculated width of the slit-like pores in the lamellar structure.

of the surfactant molecule, and have the same order of magnitude as the length of the surfactant molecules, l_s, calculated using the Tanford relation.[45] It has also been noted that the calculated mesophase surface area S_M is lower than the measured value, S_{BET}. This excess of specific surface area, ΔS, has been assigned to the existence of an interface between the ordered domains. To a first approximation the ordered domains have been assumed to be spherical with a diameter D calculated from the following equation:[36]

$$D=6/[\Delta S(1-\phi_p)\rho_s]$$

The skeletal density, ρ_s, of the oxide network measured by helium pycnometry is equal to that of amorphous silica, *i.e.* 2.2 g cm^{-3}. The pore volume fraction in the mesophase structure ϕ_p, is determined from nitrogen adsorption measurements. The calculated values of D for the hexagonal material have the same order of magnitude as the sizes determined from the width of the diffraction peaks using the Scherrer equation. For the lamellar materials, the mean calculated values are larger but in that case D depends strongly on the d_{100} and ϕ_p values.

From these results it has been shown that it is possible to direct, at room temperature, during the sol-to-gel transition, an ordered microporous structure in silica gels using lyotropic crystal mesophases as reaction media for silicon alkoxides. The different experimental values which characterise the porous texture of the final material can be correlated to calculated values assuming a polycrystalline material composed of hexagonal or lamellar domains. Remarkably, the micropore size of the calcined silica gels can be modulated by the length of the alkyl chain of the used surfactant molecules. Starting from the results obtained on ordered porous silica materials, the synthesis method was tentatively adapted to the preparation of alumina porous material. In fact aluminium alkoxides are too reactive as precursors of polymeric gels. Usually alumina colloidal gels are obtained from the destabilisation of pseudo-boehmite hydrosols. Kunitake[46] showed that a lamellar mesophase produced from a cationic surfactant can be successfully used to direct the aggregation of such colloidal alumina particles. The initial anisotropy of the material is maintained after the departure of the surfactant until the transformation into α-Al_2O_3 at high temperature. However it can be deduced from the available observations by electron microscopy that the resulting materials are expanded and highly macroporous.

We mentioned in a preliminary work[47] the possibility of alumina gel synthesis in amphiphilic media using an aluminium salt as the gel precursor. Following this method an aqueous solution of aluminium chloride (0.1 M) containing a quaternary ammonium type cationic surfactant was used to produce an aluminium hydroxide gel. After a pre-neutralisation step with ammonia (molar ratio $[NH_3]/[Al]=1$), an *in situ* controlled neutralisation was carried out by introduction of urea (molar ratio $[urea]/[Al]=1$) in the starting solution and gentle heating at 80 °C. The thermal decomposition of urea into carbon dioxide and ammonia induced an increase of the pH of the solution and the formation of the alumina gel. This kind of controlled neutralisation was previously used for the synthesis of monodispersed powders[48] and gels.[49] The main interest of this process is that it can lead to continuous and homogeneous thin layers by deposition of partially neutralised solutions

Table 3 Textural properties of the alumina gels after thermal treatment under nitrogen

Name	Heat treatment/°C	S_{BET}/m^2 g^{-1}	Pore volume/cm^3 g^{-1}	Pore size/nm
WS	450	430	0.29	2.7
8C32	450	460	0.33	2.9
14C32	450	485	0.66	5.5

and further ageing of the coatings under controlled atmosphere. The used cationic surfactants were octyl- [$C_8H_{17}(CH_3)_3N^+Br^-$] and tetradecyl- [$C_{14}H_{29}(CH_3)_3N^+Br^-$] trimethylammonium bromides. The added amounts of surfactant were determined from the analysis of the available binary diagram: tetradecyltrimethylammonium bromide–water.[50] On this diagram the weight percentage of surfactant corresponding to the boundary between the isotropic (lower wt%) and hexagonal mesophase (upper wt%) areas is located at *ca.* 32 wt%.

In contrast to silica gels, X-ray analysis carried out on a series of wet gels and on the corresponding calcined alumina gels showed that the ordered porosity formed in the wet gels cannot be maintained upon heat treatment.[47] In the case of the wet gel 8C32 ($x=8$), a main diffraction peak at 2.3 nm can be assigned to the presence of a hexagonal mesophase. In the case of the wet gel 14C32 ($x=14$), the position d of the main peak ($d<3$ nm) and the existence of another peak of lower intensity located at *ca.* $d/2$ are in favour of the presence of a lamellar mesophase. The diffraction patterns of the gels after the thermal treatment at 450 °C are consistent with that of a low temperature transition alumina.[47] The lyotropic crystal phase, present in the wet gels, has an influence on the porous texture of the calcined alumina gels (Table 3). The porous texture characteristics of gel 8C32 calcined at 450 and 800 °C are close to those of gel WS (without surfactant) calcined at 450 °C. This is a very interesting result owing to the fact that porous alumina materials, obtained by dehydration of well crystallised hydroxides, exhibit a continuous decrease of the pore size and of the surface area as the heat treatment temperature is increased. In the case of gel 14C32 the specific surface area at 450 °C is maintained at a high value but with an almost two-fold increase of pore size and pore volume compared to the reference gel WS. Unfortunately the peak located at low diffraction angle and associated with an ordered porosity for the 8C32 and 14C32 wet gels is not observed with the calcined gels. These results have been explained taking into account the low equivalent fraction of oxide (Al_2O_3) in the initial sol composition (*ca.* 3 wt% for 8C32) and the fact that the produced aluminium hydroxide gel is not a strongly cohesive gel as it is for silica. The strengthening of the inorganic network must clearly occur before the departure of the template to favour the direct templating effect of the ordered amphiphilic mesophase.

Another aspect of these templated porous textures is related to membrane applications and has to do with the anisotropy of the ordered domains in the case of supported layers. Interactions at the gel–substrate and air–gel interfaces favour the preferential orientation of the hexagonal and lamellar structures along these interfaces. Moreover the shear stress which is applied during the deposition can induce an alignment of the crystalline structures in the direction of the stress. These anisotropies are detrimental to the mass transfer performance of the final supported porous materials. In order to improve their permeability, the size of the ordered domains must be increased and ordered porous structures oriented with the resulting pores along a direction perpendicular to the layer surface. Liu *et al.*[51] showed that nanoparticle seeding favours the formation of the templating mesophases in the synthesis medium. In other respects, Fabre *et al.*[52] obtained ferrosmectics by doping swollen lamellar phases with ferrofluid nanoparticles. These hybrid mesophases can be oriented under very low magnetic field (<1 T) in comparison to the intense magnetic field (11.7 T) used recently by Tolbert *et al.*[53,54] to orient the mesophase templated silica networks.

Consistently our current approach to control the tortuosity in supported porous layers consists of the introduction of magnetic nanoparticles in the gelling solution. As a matter of fact these particles could have a seeding role in the heterogeneous nucleation of templating mesophases with an induced effect on the size of ordered domains. Moreover magnetic nanoparticles could be used to orient the mesophases. A hydrosol of maghemite (γ-Fe_2O_3) nanoparticles[55] (9.5 nm in size, ZPC = 7.3, stability pH = 2) was used as a ferrofluid source. The stability of silicon alkoxide sols in the presence of surfactant molecules and maghemite particles and the possibility to prepare ordered porous structures from these sols have been investigated recently.[56] Silica gel precursor (TMOS) and surfactant molecules $C_xH_{2x+1}(CH_3)_3N^+Br^-$ ($x=8$, 10) were used as starting materials for gel preparation. A typical weight% composition of gelling solutions is: seeding hydrosol 44, methanol 1, TMOS 8, NH_3 (0.1 M) 26, surfactant ($x=8$) 21. The seeding level in the resulting gels corresponds to 1 particle per 10^5 nm^3. Thick layers (1 mm > thickness > 0.5 mm) were deposited on flat substrates. The texture orientation of the thick layers was deduced from the variation of the X-ray diffraction peak at $d=2.45$ nm associated to the hexagonal mesophase. The peak intensities were measured at two incident angles, α between the incident beam and the substrate, β between the projection of the incident beam on the substrate and the shear stress direction of sheared wet gels. In the absence of a magnetic field during gel formation, seeded or unseeded wet gels exhibit very reproducible variations of the intensity of the diffraction peak at 2.45 nm *versus* α and β. In Fig. 15(a) the strong maximum observed for α equal to the diffraction angle θ is assigned to an alignment of the micellar cylinders and of the associated diffraction planes parallel to the surface of the substrate. The variation *versus* β, Fig. 15(b), is attributed to an alignment of the micellar cylinders along the shear stress direction. When a magnetic field (0.6 T) is applied during gel layer formation in a direction perpendicular to the surface of the substrate, no more diffraction peaks *versus* α or β are observed as expected in the case of alignment of the micellar cylinders along the magnetic field direction. Further X-ray experiments on wet gels are under way in order to confirm these results and to investigate the specific interactions between the seeding particles and the lyotropic crystal phases during gel formation.

5.0 Conclusion

The most recent advances in sol–gel processing of porous ceramic oxides have been reviewed and illustrated by recent results of our group in porous solid preparation. The current state of development of the sol–gel process allows a precise control of composition, grain structure and pore structure in ceramic oxide materials. These new developments are based on a better mechanistic control of the reactivity of precursors and derived growing species. The interplay between liquid crystal organic chemistry and the growth of inorganic frameworks provides a rare opportunity to synthesize a wide range of original structures. These systems are potentially tunable for a desired application and offer an unequalled ability for the synthesis of mesoporous and microporous materials.

Regarding both fundamental research and applications,

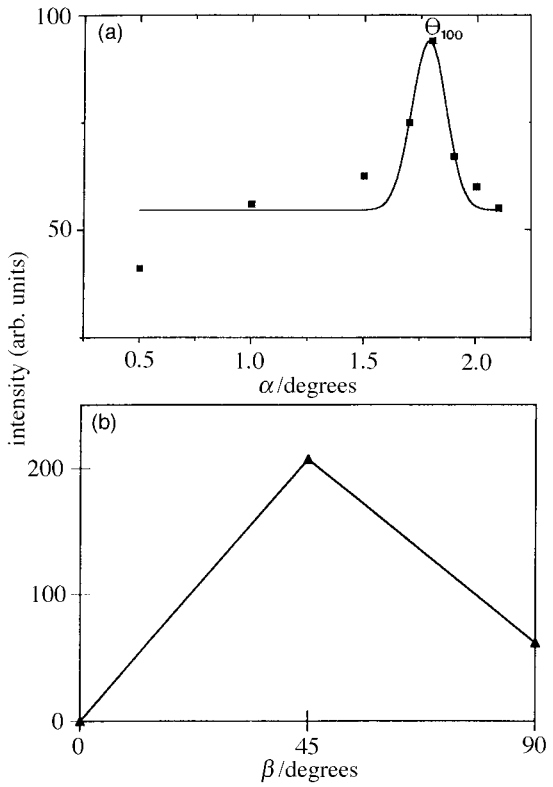

Fig. 15 X-Ray diffraction analyses on a sheared hexagonal silica layer ($x=8$). (a) Evolution of the peak intensity *versus* the incidence angle, α; (b) evolution of the peak intensity *versus* β, angle between the direction of the shear stress and that of the incidence angle.

many exciting developments are expected in the near future from sol–gel derived nanophase materials, namely for catalytic and membrane separation applications.

References

1 *Solid catalysts and porous solids*, ed. M. E. Davis and I. E. Maxwell, in *Curr. Opin. Solid State Mater. Sci.*, 1996, **1**, 54.
2 J. D. F. Ramsay and B. O. Booth, in *Fundamentals of Adsorption*, ed. A. B. Mersmann and S. E. Scholl, United Engineering Trustees Inc., 1991.
3 *Fundamentals of Inorganic Membrane Science and Technology*, ed. A. J. Burggraaf and L. Cot, Elsevier, Amsterdam, 1996.
4 *Sol–gel Science*, ed. C. J. Brinker and G. Scherer, Academic Press, New York, 1990.
5 C. J. Brinker, T. L. Ward, R. Sehgal, N. K. Raman, S. L. Hietala, D. M. Smith, D.-W. Hua and T. J. Headley, *J. Membr. Sci.*, 1993, **77**, 165.
6 C. Guizard, in *Fundamentals of Inorganic Membrane Science and Technology*, ed. A. J. Burggraaf and L. Cot, Elsevier, Amsterdam, 1996, p. 227.
7 A. J. Rubin, *Mater. Sci. Res.*, 1984, **17**, 45.
8 *Characterization of Porous Solids I, Studies in Surface Science and Catalysis Vol. 39*, ed. K. K. Unger, J. Rouquerol, K. S. W. Sing and H. Kral, *Proc. of the IUPAC Symposium (COPS I)*, Bad Soden, Germany, April 1988, Elsevier, Amsterdam, 1988.
9 *Characterization of Porous Solids II, Studies in Surface Science and Catalysis Vol. 62*, ed. F. Rodrigez-Reinoso, J. Rouquerol, K. S. W. Sing and K. K. Unger, *Proc. of the IUPAC Symposium (COPS II)*, Alicante, Spain, May 1990, Elsevier, Amsterdam, 1991.
10 *Characterization of Porous Solids III, Studies in Surface Science and Catalysis Vol. 87*, ed. J. Rouquerol, F. Rodrigez-Reinoso, K. S. W. Sing and K. K. Unger, *Proc. of the IUPAC Symposium (COPS III)*, Marseille, France, May 1993, Elsevier, Amsterdam, 1994.
11 S. Lowell and J. E. Shields, in *Powder surface area and porosity*, Chapman and Hall, London, 1984.
12 G. C. Frye, A. J. Ricco, S. J. Martin and C. J. Brinker, *Mater. Res. Soc. Symp. Proc.*, 1988, **121**, 349.
13 M. A. Fardad, E. M. Yeatman, E. J. C. Dawnay, M. Green and F. Horowitz, *J. Non-Cryst. Solids*, 1995, **183**, 260.
14 A. Ayral, A. El Mansouri, M. P. Vieira and C. Pilon, *J. Mater. Sci. Lett.*, in press.
15 C. Guizard, C. Mouchet, R. Vacassy, A. Julbe and A. Larbot, *J. Sol–Gel Sci. Technol.*, 1995, **2**, 483.
16 C. Sanchez and J. Livage, *New J. Chem.*, 1990, **14**, 513.
17 R. Vacassy, C. Guizard, V. Thoraval and L. Cot, *J. Membr. Sci.*, 1997, **132**, 109.
18 C. Sanchez, J. Livage, M. Henry and F. Babonneau, *J. Non-Cryst. Solids*, 1988, **100**, 65.
19 A. Julbe, C. Guizard, A. Larbot, L. Cot and A. Giroir-Fendler, *J. Membr. Sci.*, 1993, **77**, 137.
20 A. Pantazidis and C. Mirodatos, *11th International Congress on Catalysis, Studies in Surface Sciences and Catalysis*, ed. J. W. Hightower, W. N. Delglass, E. Iglesia and A. T. Bell, Elsevier Science B.V., Amsterdam, 1996, **101-B**, 1029.
21 A. Pantazidis, A. Auroux, J.-M. Herrmann and C. Mirodatos, *Catal. Today*, 1996, **32**, 81.
22 L. Albaric, N. Hovnanian, A. Julbe, C. Guizard, A. Alvarez-Larena and J. Piniella, *Polyhedron*, 1997, **16**, 587.
23 A. Julbe, L. Albaric, N. Hovnanian, C. Guizard, A. Pantazidis and C. Mirodatos, in *Proc. 4th Workshop of the ESF Network: Catalytic Membrane Reactors—Optimisation of Catalytic Membrane Reactor Systems*, 1997, ed. R. Bredesen, SINTEF, Oslo, pp. 215–220.
24 P. Marécot, L. Pirault, G. Mabilon, M. Prigent and J. Barbier, *Appl. Catal. B: Environment*, 1994, **5**, 57.
25 C. J. Stournaras, A. Tsetsekou, M. Muhammed, C. Guizard, A. Julbe, P. Bekiaroglou, N. Moschoudis, J. P. Joulin, D. Leonidopoulos and M. Debenedetti, in *Proc. First European Conference on Clean Cars and First Hellenic Eco Rally*, 1997.
26 C. Guizard, A. Larbot, L. Cot, S. Peres and J. Rouvière, *J. Chim. Phys.*, 1990, **87**, 1901.
27 A. Julbe, C. Balzer, J. M. Barthez, C. Guizard, A. Larbot and L. Cot, *J. Sol–Gel Sci. Technol.*, 1995, **4**, 89.
28 K. Nakanishi, Y. Yamasaki, H. Kaji, N. Soga, T. Inoue and N. Nemoto, *J. Sol–Gel Sci. Technol.*, 1994, **2**, 227.
29 S. Hansen, *Adv. Mater.*, 1993, **5**, 113.
30 C. T. Kresge, M. E. Leonowicz, W. J. Roth, J. C. Vartuli and J. S. Beck, *Nature*, 1992, **359**, 710.
31 J. S. Beck, J. C. Vartuli, W. J. Roth, M. E. Leonowicz, C. T. Kresge, K. D. Schmitt, C. T. W. Chu, D. H. Olson, E. W. Sheppard, S. B. McCullen, J. B. Higgins and J. L. Schenker, *J. Am. Chem. Soc.*, 1992, **114**, 10 834.
32 A. Monnier, F. Schüth, Q. Huo, D. Kumar, D. Margolese, R. S. Maxwell, G. D. Stucky, M. Krishnamurty, P. Petroff, A. Firouzi, M. Janicke and B. F. Chmelka, *Science*, 1993, **261**, 1299.
33 T. Dabadie, A. Ayral, C. Guizard, L. Cot, J. C. Robert and O. Poncelet, *Mater. Res. Soc. Symp. Proc.*, 1994, **346**, 849.
34 T. Dabadie, A. Ayral, C. Guizard, L. Cot, J. C. Robert and O. Poncelet, in *Proceedings of the Third International Conference on Inorganic Membranes, July 1994, Worcester, USA*, ed. Y. H. Ma, 3rd ICIM-Worcester Polytechnic Institute, Worcester, 1994, p. 411.
35 T. Dabadie, A. Ayral, C. Guizard, L. Cot, C. Lurin, W. Nie and D. Rioult, *J. Sol–Gel Sci. Technol.*, 1995, **4**, 107.
36 T. Dabadie, A. Ayral, C. Guizard, L. Cot and P. Lacan, *J. Mater. Chem.*, 1996, **6**, 1789.
37 J. E. Martin, M. T. Anderson, J. Odinek and P. Newcomer, *Langmuir*, 1997, **13**, 4133.
38 M. T. Anderson, J. E. Martin, J. Odinek, P. Newcomer and J. P. Wilcoxon, *Microporous Mater.*, 1997, **10**, 13.
39 A. Julbe, J. F. Quinson, A. El Mansouri and C. Guizard, in *Characterisation of Porous Solids IV*, ed. B. M. McEnary, T. J. Mays, J. Rouquérol, F. Rodriguez-Reinoso, K. S. Sing and K. M. Unger, The Royal Society of Chemistry, Cambridge, 1997, pp. 519–526.
40 P. Piaggio, A. Bottino, G. Capannelli, E. Carosini and A. Julbe, *Langmuir*, 1995, **11**, 3970.
41 C. Balzer, A. Julbe, A. Larbot, C. Guizard, L. Cot, J. Peureux, A. Giroir-Fendler and J. A. Dalmon, in *Proceedings of the Third International Conference on Inorganic Membranes, July 1994, Worcester, USA*, ed. Y. H. Ma, 3rd ICIM-Worcester Polytechnic Institute, Worcester, 1994, p. 629.
42 P. Scherrer, *Nachr. Göttinger Ges. Dtsch.*, 1918, **2**, 98.
43 R. H. Mikhail, S. Brunauer and E. E. Bodor, *J. Colloid Interface Sci.*, 1968, **26**, 45.
44 G. Horvath and K. Kawazoe, *J. Chem. Eng. Jpn*, 1983, **16**, 470.
45 C. Tanford, in *The Hydrophobic Effect*, 2nd edn. Wiley-Interscience, New York, 1980.

46 T. Kunitake, *Mol. Cryst. Liq. Cryst.*, 1994, **240**, 1.
47 S. Acosta, A. Ayral, C. Guizard and L. Cot, *J. Sol–Gel Sci. Technol.*, 1996, **8**, 195.
48 J. E. Blendell, H. K. Bowen and R. L. Colbe, *Am. Ceram. Soc. Bull.*, 1984, **63**, 797.
49 T. E. Wood, A. R. Siedle, J. R. Hill, R. P. Skarjune and C. J. Goodbrake, *Mater. Res. Soc. Symp. Proc.*, 1990, **180**, 97.
50 T. Warnheim and A. Jonsson, *J. Colloid Interface Sci.*, 1988, **125**, 627.
51 J. Liu, A. Y. Kim, J. W. Virden and B. C. Bunker, *Langmuir*, 1995, **11**, 659.
52 P. Fabre, C. Casagrande, M. Veyssie, V. Cabuil and R. Massart, *Phys. Rev. Lett.*, 1990, **64**, 539.
53 S. H. Tolbert, A. Firouzi, G. D. Stucky and B. F. Chmelka, *Science*, 1997, **278**, 264.
54 A. Firouzi, D. J. Schaefer, S. H. Tolbert, G. D. Stucky and B. F. Chmelka, *J. Am. Chem. Soc.*, 1997, **119**, 9466.
55 R. Massart, *IEEE Trans. Magn.*, 1991, **17**, 1247.
56 M. Klotz, A. Ayral, A. Van der Lee, C. Guizard, C. Menager and V. Cabuil, *Mater. Res. Soc. Symp. Proc.*, to be published.

Paper 8/05867I